 CMC, vol.32, no.1, pp.1-13, 2012

An Investigation on Dynamic Properties of Aluminium Alloy Foam Using Modified Large Scale SHPB Based on Dispersion Correction

H.H. Luo[1], Z.H. Tan[1,2], X. Han[1] and C. Chen[1]

Abstract: The dynamic properties of aluminium alloy foam were investigated by using split Hopkinson pressure bar (SHPB) with diameter of 40 mm. The aluminium alloy pressure bar and pulse shape technique were used to modify the traditional SHPB due to the low impedance of aluminium alloy foam. Wave dispersion correction on the aluminium alloy pressure bar was studied by Fourier series. And the finite element numerical simulation was also performed to demonstrate and validate the dispersion correction results by Fourier series method. The reflected and transmitted wave measured in SHPB experiments were corrected by the backward Fourier series expansion. The results show that there is an obvious dispersion for the stress wave travelling in the 40 mm aluminium alloy pressure bar. The dispersion correction reduces the oscillations in reflected and transmitted stress waves and stress-strain curves. And the corrected stress-strain curves of the aluminium alloy foam at various strain rates were obtained. The effects of the stain rate and strain on the dynamic properties of the aluminium foam were also discussed.

Keywords: SHPB; dispersion; dynamic properties; strain rate; aluminium alloy foam

1 Introduction

Metal foam has been widely applied in aerospace, military and civil engineering fields due to its good mechanical properties and excellent energy absorption [Gibson and Ashby (1997); Chakravarty (2010)]. Most of the application fields involve with dynamic loading such as the metal foam applied in armour, train and automobile et al. However, there is a significant difference between the dynamic and quasi-static mechanical properties of metal foams [Raj, Parameswaran, and Daniel

[1] State key laboratory of advanced design and manufacturing for vehicle body, Hunan University, Changsha, 410082, P.R. China.
[2] Corresponding Author. Email: zhtan@cqu.edu.cn. (Z.H. Tan) Tel./Fax: 00 86 731 8882 3945.

(2009)]. Furthermore, there is a considerable demanding for accuracy constitutive model from numerical simulation [Rajendran, Moorthi, and Basu (2009); Nammi, Myler, and Edwards (2010)]. Hence, it is very necessary to investigate the dynamic mechanical behavior of metal foam for use in practice and develop a specific constitutive model to characterize their deformation behavior by numerical simulation analysis.

Split Hopkinson pressure bar (SHPB) is widely used to investigate the dynamic properties of the materials at high strain rates [Zhao (2003)]. And it is based on two hypotheses: one is the one-dimensional stress wave propagation theory in elastic bar, the other one is the uniformity distribution of the stress in the specimen. Usually, a pressure bar made of steel with a small diameter (< 20 mm) is employed to satisfy the first hypothesis [Meng and Li (2003)], and pulse shaper technique is used to satisfy the other one hypothesis for brittle or soft materials testing.

Lots of work has been done on the dynamic properties of cellular materials at quasi-static, medium strain rate [Shen, Lu, and Ruan (2010); Shunmugassmy, Gupta, Nguyen, and Ceolho (2010); Wang, Shen, Lu, and Zhao (2011)] and high strain rate[Deshpande and Fleck (2000); Wang, Ma, Zhao and Yang(2006)]. However, composite materials such as concrete or foam materials need the large scale SHPB due to the uniformity distribution of the stress in the specimen [Zhu, Hu, and Wang (2009)]. It is well known that the reflected and transmitted stress waves are used to calculate the stress-strain curve of the tested materials in an SHPB experiment. The reflected wave and transmitted wave travel in the large scale pressure bar from the specimen end to the position on which the reflected and transmitted waves are measured, which is with dispersion. Thus, there are errors in the reflected and transmitted stress wave. And the dispersion correction should be done to the reflected wave and transmitted wave to ensure the reliable results when a large scale SHPB is used to investigate the dynamic compressive properties of the materials.

The dynamic mechanical properties of cellular materials depend on microstructure, density, cell size, strain rate and so on [Saha, Mahfuz, Chakravarty, Uddin, Kabir and Jeelani (2005); Krishna, Bose, and Bandyopadhyay (2007)]. It is necessary to investigate the dynamic mechanical properties of a specific foam material due to its complex mechanical properties. In the present paper, the SHPB with diameter of 40 mm was used to investigate the dynamic properties of the aluminium-silicon alloy foam. The dispersion of the stress wave in the pressure bar was studied by Fourier series, and the finite element simulation was also performed to validate the Fourier series results. Then, the dispersion correction equation was used to correct the dynamic stress-stress curves at various strain rates. And the effects of strain hardening and strain rate hardening on the flow stress were also discussed.

2 SHPB experiments

2.1 Materials and Specimens

The commercial aluminium-silicon alloy open-cell foam (JTPAL-0.75Si) used in the experiment is produced by Albert Foam Company of China. The diameter of the cell is 0.75 mm. The density of the aluminium foam is 0.864 g/cm^3, and the elastic modulus is 20 MPa. The dimension of the specimen is 30 mm in diameter and 10 mm in length.

2.2 Dynamic compressive experiments

Dynamic compressive experiments were carried out by SHPB. The diameter of the pressure bar is 40 mm. And the length of the strike bar and pressure bar is 400 mm and 2000 mm, respectively. The velocity of the strike bar is about 3.5 m/s, 4.5 m/s and 5 m/s, respectively.

The impedance of the aluminium foam is low and about 1/100 of the steel pressure bar, which would result in weak transmitted stress wave. Thus, the conventional maraging steel SHPB can't be used to test the dynamic properties of the aluminium alloy foam [Mukai, Miyoshi, Nakano, Somekawa, and Higashi (2006); Cady, Gray, Liu, Lovato, and Mukai (2009)]. Due to the mismatch of impedance, the traditional maraging steel pressure bar was replaced by the LC4 aluminium alloy pressure bar in the present paper. Furthermore, in order to ensure the equivalence of the stress in the specimen, pulse shape technique was used in the dynamic compressive experiments. A small copper with the diameter of 5 mm was used as the pulse shaper to ensure the stress equivalence in the specimen. And Semi-conductor strain gauge was used to record the transmitted wave, which can improve the signal to noise level.

The typical stress wave obtained by traditional and modified SHPB in the experiments was shown in Fig. 1.

3 Dispersion Analysis

It is well known that the dispersion effect should be considered when the stress wave propagates in a large scale bar [Merle and Zhao (2006); Aleyaasin and Harrigan (2010)]. To analyze the dispersion, Fourier series was used to investigate the dispersion of the stress pulse in the 40 mm aluminium alloy pressure bar, and the results were validated by finite element method.

The schematic graph of the analytical model was shown in Fig. 2. A trapezoid pulse is applied at the front end of the pressure bar.

It is well known that an arbitrary stress pulse can be fit by the Fourier series as

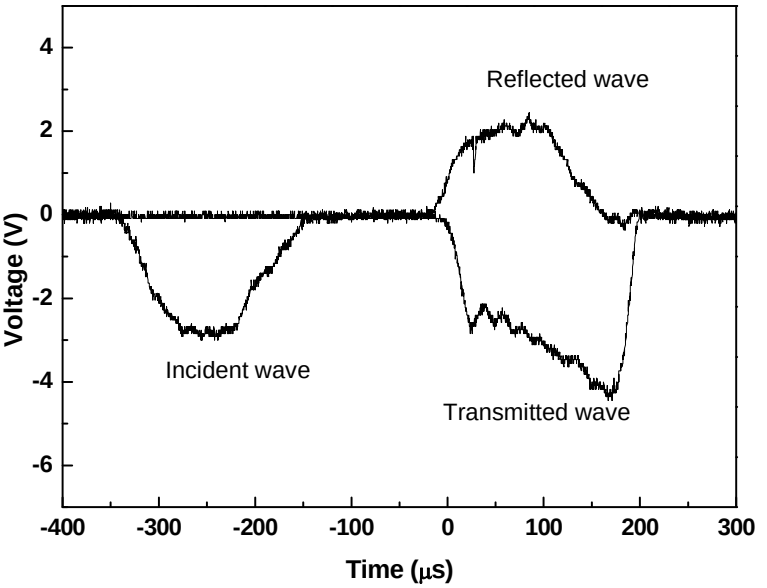

Figure 1: Typical SHPB stress wave in the experiments.

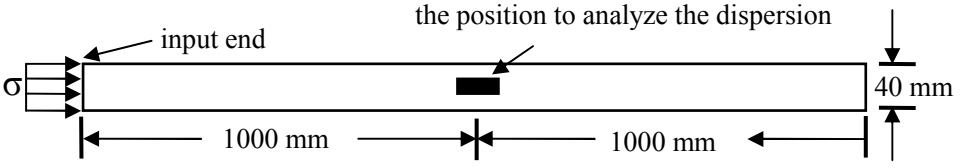

Figure 2: Schematic graph of input pressure bar for analytical model.

shown in Eq. (1). And it means that the applied pulse consists of n harmonic waves. In the present paper, the number of Fourier components n is 50, which has been demonstrated by Gong et al.[Gong, Malvern, and Jenkins (1991)].

$$F(t) = \sum_{n=0}^{N} \left[A_n \cos(n\omega_0 t) + B_n \sin(n\omega_0 t) \right] \tag{1}$$

Each component has the different wave length and frequency, which is corresponding to wave speed (c_n). The Pochhammer-Chree equation [Gong, Malvern, and Jenkins (1991)] is used to solve the relationship between wave length (λ_n) and wave speed (c_n), which includes the non-dimensional variables of phase velocity (wave speed c_n), wave length (λ_n), Poisson's ratio (υ_n), elastic modulus and diameter of the cylinder (d). The equation is expressed as

$$\frac{c_n}{c_0} = f\left(\frac{d}{\lambda_n}, \upsilon\right) \tag{2}$$

Where $c_0 = \sqrt{E/\rho}$ is the elastic wave velocity, c_n is the wave speed of the nth component, f is a certain nonlinear function, d is the diameter of the pressure bar, λ_n.is the wave length of the nth component, υ is the Poisson's ratio.

For a given Poisson ratio, Eq. (2) can be solved. And Bancroft [Bancroft (1941)] has solved the Eq. (2) for a series of Poisson's ratio. For a specific Poisson's ratio, the roots of Eq. (2) can be interpolated from data in Table 1.

Table 1 shows the data solved by Bancroft for Poisson's ratios 0.30 and 0.35 and the interpolated value for Poisson's ratio 0.33 (The Poisson's ratio of the pressure bar is 0.33). Based on these numerical results, the phase velocity c_n/c_0 corresponding to any wave length d/λ_n can be obtained. An algebraic formula that fits data for a specific Poisson's ratio in Table 1 [Gong, Malvern, and Jenkins (1991)], the formula can be expressed as

$$\left(\frac{c_n}{c_0}\right) = 0.5764 + 0.4236 / \left[\sum_{m=2}^{M} D_m (d/\lambda_n)^m + D_1 (d/\lambda_n)^{1.5} + 1 \right] \tag{3}$$

According to Eq. (3), $D_1, D_2, D_3 \cdots\cdots D_M$ was obtained by a nonlinear least square curve fitting method to fit the data of Poisson's ratio 0.33 in Table 1. When M = 8, the constant obtained are D_1 = 12.0142, D_2 = -44.2666, D_3 = 99.2829, D_4 = -34.4045, D_5 = -178.0848, D_6 = 66.3077, D_7 = 275.4951, D_8 = -190.2569.

The relationship between the phase velocity c_n and frequency f_n for the nth component is

$$c_n = f_n \lambda_n = (n\omega_0/2\pi)\lambda_n \tag{4}$$

Table 1: c_0/c_n as a function of d/λ_n and υ

d/λ_n	ν				
	0.25	0.30	0.33*	0.35	0.40
0	1.00000	1.00000	1.00000	1.00000	1.00000
0.05	0.99961	0.99944	0.99932	0.99924	0.99901
0.10	0.99843	0.99774	0.99726	0.99694	0.99602
0.15	0.99638	0.99482	0.99374	0.99302	0.99097
0.20	0.99333	0.99054	0.98861	0.98732	0.98373
0.25	0.98909	0.98466	0.98167	0.97967	0.97418
0.30	0.98337	0.97691	0.97264	0.96979	0.96214
0.35	0.97572	0.96688	0.96119	0.95739	0.94747
0.40	0.96559	0.95410	0.94695	0.94218	0.93007
0.45	0.95220	0.98310	0.92962	0.92397	0.91001
0.50	0.93479	0.91854	0.90908	0.90277	0.88758
0.55	0.91288	0.89549	0.88559	0.87899	0.86333
0.60	0.88681	0.86964	0.85990	0.85341	0.83806
0.65	0.85800	0.84222	0.83314	0.82709	0.81265
0.70	0.82841	0.81466	0.80652	0.80110	0.78792
0.75	0.79982	0.78818	0.78106	0.77632	0.76452
0.80	0.77332	0.76357	0.75741	0.75330	0.74284
0.85	0.74943	0.74125	0.73592	0.73236	0.72310
0.90	0.72826	0.72130	0.71665	0.71355	0.70532
0.95	0.70967	0.70365	0.69955	0.69682	0.68946
1.00	0.69344	0.68814	0.68447	0.68203	0.67537
1.20	0.64712	0.64321	0.67348	0.63869	0.63368
1.40	0.62048	0.61687	0.66249	0.61284	0.60844
1.60	0.60479	0.60111	0.65149	0.59713	0.59289
1.80	0.59526	0.59139	0.64050	0.58731	0.58304
2.00	0.58932	0.58524	0.63399	0.58101	0.57664

* The data for 0.33 in the column was obtained by interpolating.

Equation (4) can be non-dimensionalized, and gives

$$\left(\frac{c_n}{c_0}\right)\left(\frac{d}{\lambda_n}\right) = \left(\frac{n\omega_0}{2\pi}\right)\left(\frac{d}{c_0}\right) \tag{5}$$

Combining with Eq. (3) and (5), $c_1, c_2, c_3 \cdots\cdots c_n$ can be solved. If no dispersion, the whole pulse would travel distance z along the bar at the wave velocity c_0 in time z/c_0. However, the different component waves travel distance z along the bar at the

corresponding velocity c_n in time z/c_n. According to Eq. (1), when the component wave travels distance z in the bar, the phase angle difference of nth component in comparison with the component wave travelling with no dispersion will be

$$\Delta\phi = n\omega_0\Delta t = n\omega_0\left(\frac{z}{c_0} - \frac{z}{c_n}\right) \tag{6}$$

Where, z is the distance travelled by the component wave in the bar.

After the pulse travels distance z along the bar, the pulse at position z can be constructed by the Fourier series as

$$F(t) = \sum_{n=0}^{N}\left[A_n\cos(n\omega_0 t + \Delta\phi) + B_n\sin(n\omega_0 t + \Delta\phi)\right] \tag{7}$$

If the pulse travels in the bar with dispersion, the dispersed pulse can be constructed by Eq. (7) at any position in the bar.

The numerical simulation was also performed to analyze the dispersion and validate the results of Eq. (7). The dimension of the finite element model is the same with that in Fig. 2. And a pulse was applied at the front end of the bar. The duration time is 120μs and the amplitude is 800 MPa. The pulse at distance z =1000 mm was constructed by Eq. (1) to (7). The material of the pressure bar is LC4 aluminium alloy. The elastic modulus is 71 GPa, and the density is 2.71×10^3 kg/m^3. The Poisson's ratio is 0.33. The procedures of demonstration and validation are as following:

(1) The Fourier series with n=50 components were used to construct the pulse according to Eq. (1).

(2) Interpolate the data for Poisson's ratio 0.33, and then coefficients of Eq. (3) were obtained by the nonlinear least square fitting method.

(3) Combining with Eq. (3) and (5), the wave length and the corresponding speed were solved. And then, the phase angle difference for each component was calculated by Eq. (6).

(4) Construct the pulse at the position of the distance z =1000mm by Eq. (7).

And the 3D finite element numerical simulation was performed by LSDYNA. The pulse was applied at the front of the bar. The pulse at the position z=1000mm was obtained compared with the results of Eq. (7). The results were shown in Fig. 3.

Figure 3 illustrates the pulse with dispersion at the position of z = 1000 mm in the bar. There is an obvious oscillation when the input stress wave propagates along the pressure bar in comparison with the origin input stress wave. And the analytical results of Eq. (7) agree well with finite element results. Thus, Eqs. (1) to (7) can be used to correct the stress wave in the pressure bar.

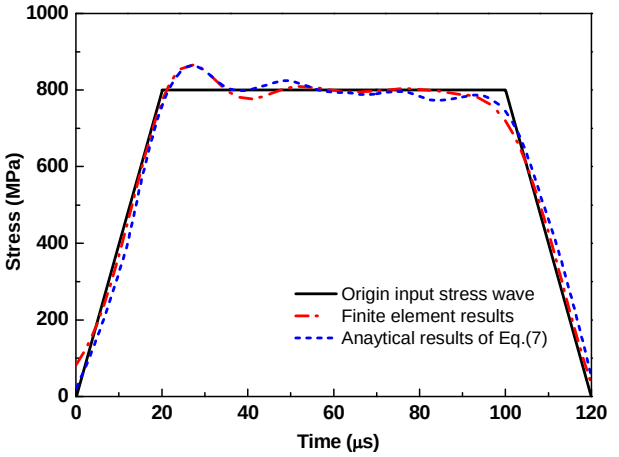

Figure 3: Validation of the analytical solution of Eq. (7).

The reflected wave and transmitted wave recorded by the strain gauges are the stress waves that travel from the front and rear ends of the specimen with dispersion. We need to obtain the pulse before travelling with dispersion. Eq. (7) is used to solve forward-dispersion-correction. The reflected wave and transmitted wave corrections are the backward-dispersion-correction. The change of phase angle should be backward. So, the Eq. (1) should be revised as

$$F(t) = \sum_{n=0}^{N} \left[A_n \cos\left(n\omega_0 t - \Delta\phi\right) + B_n \sin\left(n\omega_0 t - \Delta\phi\right) \right] \tag{8}$$

4 Results and discussions

4.1 Experimental results and Corrections

Equation (8) is used to correct the reflected and transmitted wave measured in SHPB experiments. And the measured and corrected reflected and transmitted stress waves were shown in Fig. 4. According to the principle of SHPB, uncorrected and dispersion-corrected stress-strain curves of the specimen were calculated by corresponding reflected and transmitted stress wave in Fig. 4.

Figure 5 illustrates the uncorrected and dispersion-corrected stress-strain curves of aluminium-silicon alloy foam at various strain rates. Compared to the uncorrected stress-strain curves, dispersion-correction reduces oscillation of the stress-strain curves. Less oscillation makes the results more accuracy. It is evident that the strain rate has a significant effect on flow stress from Fig. 5. For these tested

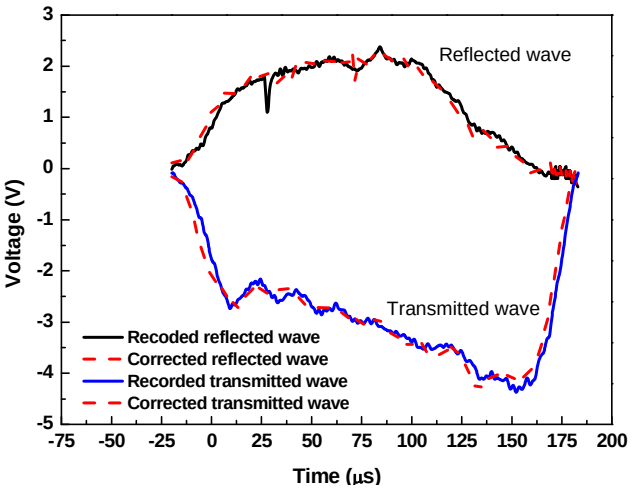

Figure 4: Typical uncorrected and dispersion-corrected reflected wave and transmitted wave.

samples, the flow stress at high strain rate increases considerably as compared to under quasi-static loading before the densification step. There are obvious three steps (elastic step, plateau step and densification step) in the curves. The plateau stress increases with the increase of the strain rate, while the densification decreases with the increase of the strain rate.

4.2 Strain rate sensitivity

Figure 6 illustrates the variation of flow stress with strain rate at given plastic strain ranging from 10% to 20%. It can be seen that the curves parallel with each other. For a given strain rate, the increase of flow stress by strain-hardening is about 0.9 MPa; for a given strain, the increase of flow stress by strain rate hardening is about 3.5 MPa. Thus, the effect of the strain rate on the flow stress is larger than strain hardening does.

The aluminium-silicon alloy foam is a strain rate sensitive material. And the strain rate sensitivity can be express as

$$R = \frac{\sigma_d - \sigma_s}{\sigma_s} \frac{1}{\ln(\dot{\varepsilon}_d/\dot{\varepsilon}_s)} \tag{9}$$

Where σ_d is the dynamic yield stress, σ_s is the quasi-static yield stress, $\dot{\varepsilon}_s$ and $\dot{\varepsilon}_d$ are the quasi-static and dynamic strain rate, respectively.

The strain rate sensitivity is 0.081, 0.124 and 0.174 corresponding to 1400/s, 2000/s and 2500/s, respectively. It increases with the increasing of the strain rate.

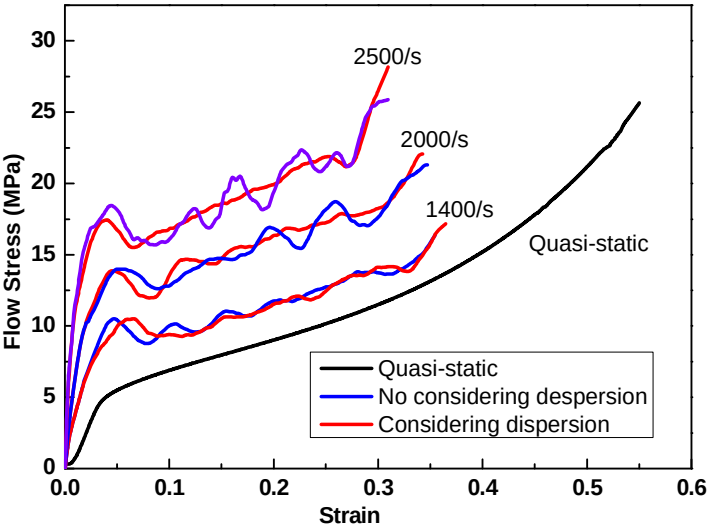

Figure 5: Uncorrected and dispersion-corrected stress-strain curves at various strain rates.

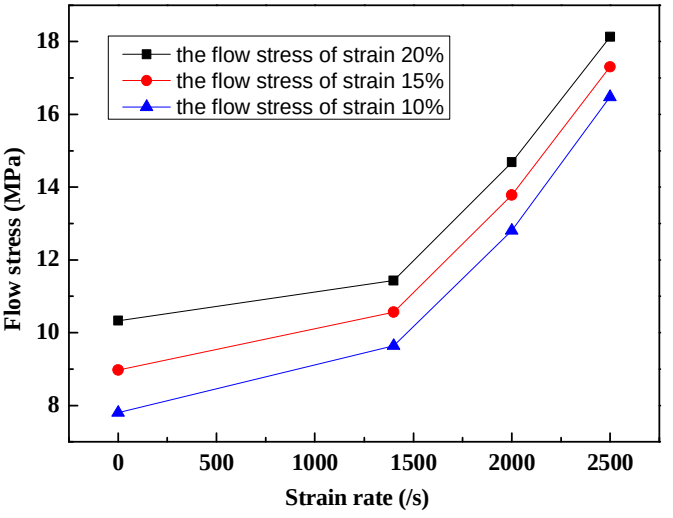

Figure 6: Variation of flow stress with strain rate at given plastic strain for aluminium-silicon alloy foam

5 Conclusions

The SHPB experiments were carried out to investigate the compressive properties of aluminium-silicon alloy foam. The pressure bar is made of LC4 aluminium alloy and the diameter is 40mm. The dispersion of stress wave in the pressure bar was analyzed by Fourier series. And the finite element analysis was also performed to demonstrate and validate the results of Fourier series. And the Fourier series results agree well with finite element results. The results show that there is obvious dispersion for the stress wave travelling in the LC4 aluminium alloy pressure bar with the diameter of 40 mm.

Then, the dispersion correction technique by Fourier series was used to correct the reflected and transmitted stress wave measured in SHPB experiments. The results show that there are the fewer oscillations in the dispersion-corrected stress-strain curves compared with the uncorrected stress-strain curves. And the strain rate has a significant effect on the plateau stress of the open-cell aluminium silicon alloy foam. Moreover, the effect of the strain rate on the flow stress is larger than strain hardening does.

Acknowledgement: The work is supported by the National Natural Science Foundation of China (No. 11202071) and the Special Fund for Basic Scientific Research of Central Colleges of China. The financial contribution is gratefully acknowledged.

References

Aleyaasin, M.; Harrigan, J.J.(2010): Wave dispersion and attenuation in viscoelastic polymeric bars: Analysing the effect of lateral inertia. *Int. J. Mech. Sci.,* Vol. 52, No. 5, pp. 754-757.

Bancroft, D. (1941): The Velocity of Longitudinal Waves in Cylindrical Bars, *Phys. Rev.*, Vol. 59, pp. 588-593.

Cady, C.M.; Gray III, G.T.; Liu, C.; Lovato, M.L.; Mukai, T.(2009): Compressive properties of a closed-cell aluminium foam as a function of strain rate and temperature. *Mater. Sci. Eng. A,* Vol. 525, No. 1-2, pp. 1-6.

Chakravarty, U.K. (2010): An investigation on the dynamic response of polymeric, metallic, and biomaterial foams. *Compos. Struct.*, Vol. 92, No. 10, pp. 2339-2344.

Deshpande, V.S.; Fleck, N.A. (2000): High strain rate compressive behavior of aluminium alloy foam. *Int. J. Impact Eng.*, Vol. 24, No. 3, pp. 277-298.

Gibson, L.J.; Ashby, M.F. (1997): Cellular solids: structure and properties. *Cam-*

bridge University Press.

Gong, J.C.; Malvern, L.E.; Jenkins, D.A. (1991): Dispersion investigation in the split Hopkinson pressure bar, *J. Eng. Mater. Technol.*, Vol. 112, pp. 309-314.

Krishna, B.V.; Bose, S.; Bandyopadhyay, A. (2007): Strength of open-cell 6101 aluminum foams under free and constrained compression. *Mater. Sci. Eng. A*, Vol. 452-453, pp. 178-188.

Merle, R.; Zhao, H. (2006): On the errors associated with the use of large diameter SHPB, correction for radially non-uniform distribution of stress and particle velocity in SHPB testing. *Int. J. Impact Eng.,* Vol. 32, No. 12, pp. 1964-1980.

Mukai, T.; Miyoshi, T.; Nakano, S.; Somekawa, H.; Higashi, K. (2006): Compressive response of a closed-cell aluminum foam at high strain rate. *Scripta Mater.*, Vol. 54, No. 4, pp. 533-537.

Meng, H.; Li, Q.M. (2003): An SHPB set-up with reduced time-shift and pressure bar length. *Int. J. Impact Eng.*, Vol. 28, No. 1-2, pp. 677-696.

Nammi, S.K.; Myler, P.; Edwards, G. (2010): Finite element analysis of closed-cell aluminium foam under quasi-static loading, *Mater. Design*, Vol. 31, No. 2, pp. 712-722.

Raj, E.R.; Parameswaran, V.; Daniel, B.S.S. (2009): Comparison of quasi-static and dynamic compression behavior of closed-cell aluminum foam. *Mater. Sci. Eng. A*, Vol. 526, No. 1-2, pp. 11-15.

Rajendran, R.; Moorthi, A.; Basu, S.(2009): Numerical simulation of drop weight impact behaviour of closed cell aluminium foam. *Mater. Design*, Vol. 30, No. 8, pp. 2823-2830.

Saha, M.C.; Mahfuz, H.; Chakravarty, U.K.; Uddin, M.; Kabir, Md. E.; Jeelani, S. (2005): Effect of density, microstructure, and strain rate on compression behavior of polymeric foams. *Mater. Sci. Eng. A*, Vol. 406, No. 1-2, pp. 328-336.

Shen, J.H.; Lu, G.X.; Ruan, D. (2010): Compressive behavior of closed-cell aluminium foams at high strain rates. *Compos. Part B: Eng.,* Vol. 41, No. 8, pp. 678-685.

Shunmugasamy, V.C.; Gupta, N.; Nguyen, N.Q.; Ceolho, P.G. (2010): Strain rate dependence of damage evolution in syntactic foams, *Mater. Sci. Eng. A,* Vol. 527, No. 23, pp. 6166-6177.

Wang, Z.H.; Shen, J.H; Lu, G.X.; Zhao, L.M. (2011): Compressive behavior of closed-cell alminium alloy foams at medium strain rates. *Mater. Sci. Eng. A,* Vol. 528, No. 6, pp.2326-2330.

Wang, Z.H.; Ma, H.W.; Zhao, L.M.; Yang, G.T. (2006): Studies on the dynamic compressive properties of open-cell aluminium alloy foams. *Scripta Mater.,* Vol.

54, No. 1, pp. 83-87.

Zhao, H. (2003): Material behavior characterization using SHPB techniques, tests and simulations. *Comput. Struct.,* Vo. 81, No. 12, pp. 1301-1310.

Zhu, J.; Hu, S.S.; Wang, L.L. (2009): An analysis of stress uniformity for concrete-like specimens during SHPB tests. *Int. J. Impact Eng.,* Vol. 36, No. 1, pp. 61-72.